International Journal of Engineering Trends and Technology
ISSN: 2231–5381 / https://doi.org/10.14445/22315381/IJETT-V72I3P119

Volume 72 Issue 3, 208-217, March 2024

Original Article

Methods for Analyzing Robotic Systems Made of Composite Materials

Kamil Khayrnasov

Moscow Aviation Institute (National Research University), Moscow, Russian Federation.

Corresponding Author : khayrnasov_mai@mail.ru

Received: 09 September 2023 Revised: 27 January 2024 Accepted: 19 February 2024 Published: 17 March 2024

Abstract - *Methods for modeling, calculation, and analysis of robotic systems are given in the example of a dynamic of stand. A three-layer structure of a dynamic of the stand made of external load-bearing 8-layer composite materials and filler between the load-bearing layers is considered. Elements of movement of robotic systems such as bearings, gearboxes, and gear rims are modeled as a system of rod systems of identical rigidity. An algorithm and a program for calculating the stiffness of gearboxes, gear rims, bearing supports, and engines were developed. The influence of the location of the base layers of the composite material on the stress state of the stand under dynamic loading is considered. The problem is solved by the finite element method. The convergence of the calculation results was checked by increasing the number of finite elements and comparing the results obtained. To achieve maximum rigidity and strength of the stand, a method has been developed to arrange the base of the composite material layers along the lines of maximum stresses. As a result of the calculations, the stress-strain state of the stand materials was obtained. The criteria for the destruction of layered materials were used to assess the bearing capacity of a stand made of composite material under dynamic loading. The conducted studies are applicable to a wide class of robotic structures made of composite material under dynamic impact.*

Keywords - *Robotic systems, Composite materials, Dynamic loads, Finite element method, Stress-strain state, Failure criteria.*

1. Introduction

Robotic systems are becoming more widespread in dentistry, logistics, assembly and sorting [1-5]. The use of robotics has increased due to the development of computer technologies: artificial intelligence and computer vision. Therefore, it is important to develop a methodology for calculating and analyzing such systems, which is the goal of this work. For manufacturing dynamic systems, using materials with high specific strength characteristics is important. Since the inertial characteristics of robotic systems affect positioning accuracy, which is one of the important characteristics of robotic systems. One of these materials is a composite, widely used in aviation, mechanical engineering, etc. The composite material changes its characteristics depending on the orientation of the layers for the layers of a multilayer composite material. Therefore, it is important to consider different combinations of layers and determine the composite material of maximum strength. In this article, the arrangement of layers of maximum strength is determined. The stand under consideration has all the attributes of robotic systems, bearings, gear rims, gearboxes, motors and moving elements [6-10]. Identifying such elements in the finite element method is a complex task that requires a large amount of theoretical and experimental research in the design and manufacturing process. To determine the stiffness of such elements, an algorithm and a program for calculating the stiffness of such elements were developed. In the finite element approximation, bearings, gear rims, gearboxes, and motors were replaced by a system of rod elements of identical rigidity. Failure criteria are used to determine the load-bearing capacity of laminated materials. In this study, the most common failure criteria are applied: Tsai-Wu, Tsai-Hill, and Hoffman criteria [11-14]. A significant number of works have been devoted to the calculation of structural elements made of composite materials under dynamic loading [15-21]. At the same time, the calculation of the structure as a whole is not enough. Therefore, developing methods for calculating and analyzing robotic systems is an important and urgent problem. Comparison with existing studies in the literature is difficult due to the complex problems solved in this article: dynamics, moving elements, and parts that support them (bearings, ring gears, and gearboxes). In computer-aided design systems, there is an interpretation of such elements, mainly in the form of nodal points. However, at the same time, the element's scale and the stiffness from the bearing plane are not taken into account. There is no algorithm for calculating structures for dynamic loads. Currently, there have been no studies of stands made of composite material and the influence of the number of layers of composite material and their orientation on the stress-deflation state of the robotic system, stand for semi-

natural modeling. This article presents methods for calculating robotic systems: semi-natural modeling stands made of composite materials under dynamic loading. An eight-layer composite material is considered. A study of the orientation of the base of an eight-layer composite material on the stress-strain state of the stand under dynamic loading is being conducted, which makes it possible to obtain a structure of maximum rigidity and strength. Considering that the criteria for the destruction of multilayer materials are based on the fact that the destruction of one layer of a multilayer material leads to the destruction of the material as a whole. The strength and rigidity characteristics of the material affect the positioning accuracy of the robotic structure, one of the main characteristics affecting the performance of the robotic structure. Strength characteristics are determined under various destruction criteria of a multilayer composite material. The methods developed in the article make it possible to study the performance of robotic systems, which are becoming increasingly widespread in many areas.

2. Materials and Methods

2.1. Relation Between Stresses-Strains

There are two approaches to solving the problems of structures made of composite material. The first method is to determine the reduced characteristics of the laminate. It is necessary to obtain a material with orthotropic characteristics and solve the problem of a homogeneous orthotropic material. In this case, the characteristics of the material are determined by equations.

The second approach is associated with solving the problem, taking into account the characteristics of each layer of the multilayer material, while the number of resolving equations increases by the number of layers of the multilayer material used. In this study, the second method is used since the failure criteria take into account the stress-strain state of each layer.

2.2. Method for Obtaining the Most Durable Structure

The composite material has properties that change its characteristics depending on the base's location in the layers of the multilayer composite material [22-24]. The composite material whose base layer coincides with the direction of the load has the greatest strength. However, this approach is valid for uniaxial loading. In the case of a complex stress-strain state, it is necessary to conduct studies to determine the trajectories of maximum stress and arrange the base of the layers of the composite material along these trajectories. In this case, as a first approximation, it is necessary to obtain a structure of maximum rigidity and strength. In the general case, it is necessary to arrange the layers at an angle to the maximum stresses to perceive shear stresses. The stresses act perpendicular to the main stresses. The layer-by-layer stress-strain state and use of the failure criteria are considered to determine the structure of the composite material of maximum strength and rigidity. In the present paper, such studies were carried out, and the angles of the base of the composite material were determined by layers, allowing the maximum rigidity and strength of the structure to be achieved.

2.3. Method for Determining the Structure of a Composite Material

Approximation of elements of robotic systems such as bearings, gearboxes, gear rims, and motors is a complex task requiring a large amount of theoretical and experimental research. In the present study, an algorithm and a program for calculating the stiffness characteristics of these elements have been developed. In the finite element approximation, such elements in the stand were replaced by a chain of rod systems of identical rigidity. Such a replacement is justified since the calculations carried out to determine the natural frequencies of the benches corresponded to the experimental results. Below is an algorithm for determining the rigidity characteristics of gearboxes, bearings, and gear rims.

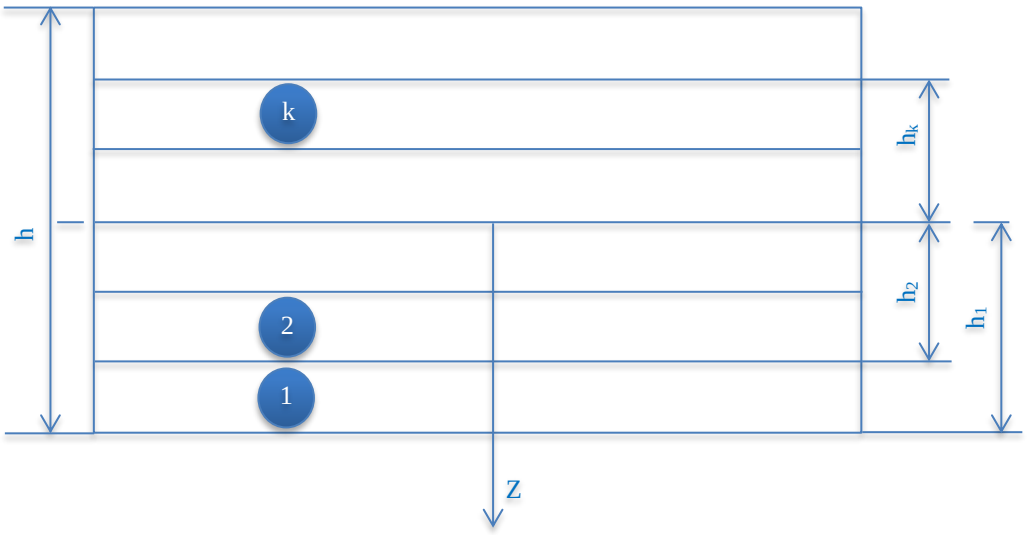

Fig. 1 Multilayer composite material

2.4. Simulation and Approximation of the Stand

The stand has a three-stage structure (Figure 1). To calculate the stand, it is necessary to simulate it. The bench approximation by finite elements is carried out [25-29]. To enhance the rigidity and strength of the stand design, the stand was made in the form of a three-layer structure, consisting of external bearing layers of 8-layer composite material and a filler of lightweight material in the form of foam that perceives shear stresses and prevents the bearing layers from approaching. The technology for modeling the three-layer structure of the stand was as follows. The simulation of the stand was carried out, and the stand models were assigned the aggregate characteristics. Design tools formed shells on the outer surface of the model, which were assigned the characteristics of an 8-layer composite material. Bearings, gear rims and gearboxes were approximated by a rod system of identical rigidity. The refinement of the finite element label checked the validity of the calculation results.

2.5. Stiffness Calculation Algorithm

The algorithm for calculating the stiffness of the gearbox is carried out according to the formulas of the theory of machines and mechanisms. Some of the main parameters that must be taken into account when operating a gearbox are stiffness, gear ratio, and natural frequency. The stiffness of the gearbox can be determined experimentally and theoretically. If the experimental data are not subject to change, then the program for determining the stiffness of the gearbox allows determining the stiffness of an arbitrary gearbox. Experimental data, in this case, serve to verify the reliability of the algorithm and the program for calculating the gearbox. In this study, an algorithm and a program for calculating the gearbox in the Microsoft Excel environment were developed. The program determines the necessary parameters of the gearbox, including the rigidity of the gearbox as a whole. Theoretically, the results obtained using the program were tested by experimental data; the difference in the results was 10%, which is an acceptable value for devices whose rigidity depends on many parameters. Also, with the program's help, the stiffness of bearings and gear rims were determined. Figure 2 shows a kinematic diagram of the reducer.

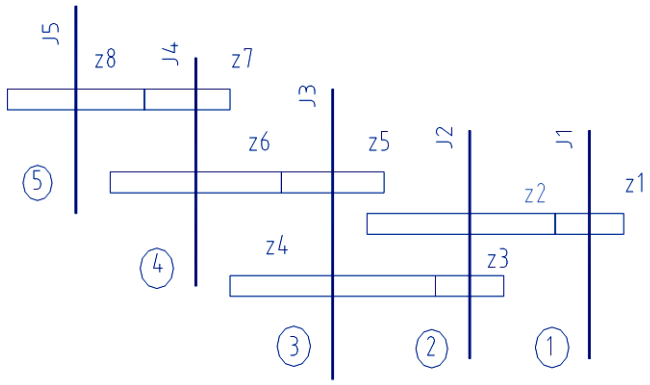

Fig. 2 Kinematic diagram of the reducer

2.6. Initial Parameters

Moments of inertia of gear shafts J_5, J_4, J_3, J_2, J_1 ($kg \times m \times s^2$), angular velocity υ_5 ($\frac{1}{s}$), angular acceleration ω_5 ($\frac{1}{s^2}$)and frequency f(Hz).

Gear ratios $i54 = z8 \div z7, i43 = z6 \div z5, i32 = z4 \div z2, i21 = z2 \div z1, i11 = z1 \div z1.$

Gear ratios related to the input shaft $i51 = i54 \times i43 \times i32 \times i21 \times i11, i41 = i51 \div i54, i31 = i41 \div i43, i21 = i31 \div i32, i11 = i21 \div i11.$

Total gear ratio $i_{tot} = i54 \times i43 \times i32 \times i21 \times i11$.

Gear ratio of the gearbox $i_{red} = i43 \times i32 \times i21 \times i11.$

Moments of inertia about to input shaft $J51 = J5 \div i51^2, J41 = J4 \div i41^2, J31 = J3 \div i31^2, J21 = J2 \div i21^2, J11 = J1 \div i11^2.$

Shaft accelerations $\omega_4 = \omega_5 \times i54, \omega_3 = \omega_4 \times i43, \omega_2 = \omega_3 \times i32, \omega_1 = \omega_2 \times i21.$

Shaft torques $M5, M5, M4 = J4 \times \omega_4 + M5/i54, M3 = J3 \times \omega_3 + M4/i43, M2 = J2 \times \omega_2 + M3/i32, M1 = J1 \times \omega_1 + M2/i21.$

2.7. Shaft Load

$R_{ocr} = M_j \div m \times z, P_{rad} = R_{ocr} \times \tan 20°$, where m is the modulus, z is the number of teeth, and M_j is the moment on the shaft.

The reactions of the supports R_1 and R_2 are determined by the formulas of resistance of materials, taking the moment of inertia of the shaft section Jshaft=$3.14 \times Deq^4/64$ $J_{shaft} = 3.14 \times Deq^4 \div 64$ in terms of Deqv equivalent to a constant bending diameter.

At the points of application of forces and supports, displacements and angles of rotation are determined by the BEAM program.

2.8. Deformation of the Bearing from Fit on the Shaft and into the Housing

$g_r = g_{r0} - \Delta d_1 - \Delta D_2$, where g_{r0} is the initial clearance of the ball bearing, Δd_1 is the increase in the outer diameter of the inner ring from the fit on the shaft, ΔD_2 is the decrease in the inner diameter of the outer ring from the fit into the housing determined from the graphs [9], depending on the ratio of the stiffness of the mating parts:

- shaft (steel) $S_v = d_2 \div d$, bearing inner ring $S_{vn} = d \div d_1$, bearing outer ring $S_H = d \div d_1$, body (steel) $S_k = D \div D_1$, where d_2 is the bore of the hollow shaft, d is the

inner diameter of the bearing inner ring and, d_1 is the outer diameter of the bearing inner ring, D, D_2, respectively, are the outer and inner diameter of the outer ring of the bearing, D_1 is the outer diameter of the housing;

- ratios of deformations and fitting interferences in shaft-inner ring connections $d_1 \div H_b$, housings with outer ring $D_2 \div H_k$, $H_b = H_{av} - H_1$, H_{av} is the average value of the fit interference of the inner ring of the bearing, H_1 is the amount of unevenness and $H_k = H_{av} - H_1$, also for the outer ring of the bearing.

D_1 is the increase in the outer diameter of the inner ring, and D_2 is the reduction of the inner ring's outer diameter.

2.9. Bearing Deformation under Load

$\delta_r = \delta_{r1} + \delta_{r2}$, where δ_{r1} is the deformation in contact of the most loaded rolling element with the raceway in the bearing, δ_{r2} is the radial compliance in contact with the bearing rings with the shaft and housing mounting surfaces. Deformation in contact of the most loaded rolling element with the raceway in the bearing:

- With preload:
  $\delta_{r1} = \beta \times \delta_{r0}$;
- With radial clearance:
  $\delta_{r1} = \beta \times \delta_{r0} - \frac{gr}{2}$.

The coefficient β, which takes into account the amount of interference or clearance in the bearing, is determined from the graphs [8]. The value of δ_{r0} for bearings of various types can be determined from the equations [8]:

- For single-row ball:
  $\delta_{r0} = 2.0\times10^{-3} \times \sqrt[3]{\frac{Q_0^2}{D_T}}$;
- For angular contact tapered bearing:

$\delta_{r0} = 6.0\times10^{-4} \times \frac{Q_0^{0.9}}{\cos\alpha \times l^{0.8}}$, where $Q_0 = \frac{5\times R}{i\times z\times\cos\alpha}$, R is the radial load on the support, i are the number of rows of rolling elements, z is the number of rolling elements in one row, $\alpha = \arccos(1 - \frac{gr}{2}\times A), \alpha$ is the contact angle, D_T is the ball diameter, $d_{el} = 0.5232 \times D_T$ is the groove diameter $A = D_T \times (2 \times d_{el} \times D_T - 1)$.

2.10. Radial Compliance in Contact of Bearing Rings with Shaft and Housing Seating Surfaces

$\delta_{r2} = \frac{4\times R\times k}{\pi\times d\times B}\left(1 + \frac{d}{D}\right)$, where $k = \frac{0.015\text{mm}^2}{kg}$, D, d and B are the outer and inner diameters of the bearing and its width, respectively.

2.11. Calculation of the Rotation of the Gear Wheel Caused by the Elastic Deflection of the Shaft

$\varphi_{defl} = \frac{2}{m\times Z} \times (w_{circ} + w_{rad} \times tg20^o)$, where w_{circ} and w_{rad} are the values of the shaft deflections in the middle plane of the transmission, respectively, taking into account deformations and movements in the bearings, Z is the number of teeth in the gear, and m is its module.

2.12. Calculation of Error Due to Shaft Twist

$\varphi_{tw}=\sum(M\times li/(G\times Jp)$, radian, where G are the shear modulus, $Jp=\pi\times(D^4-d^4)/32$ is the polar moment of inertia, li is the length of twisted section, M is the moment on the shaft.

2.13. Calculation of the Error Caused by the Compliance of the Ring Gear

$\varphi_{tooth}=M/(k\times d^2\times b)$, radian, where d is the pitch diameter of the gear rim, b is the working width of the gear rim, and $k=368\text{kg/mm}^2$ is the experimental coefficient.

2.14. Calculation of Error Due to Keyed Connection

$\varphi_{shp}=M/k_{shp}\times d_b^2\times l\times h\times z$, radian, where d_b is the shaft diameter, l is the working length of the key, h is the height of the key, z is the number of keys, $k_{shp}=15\text{kg/mm}^3$ for parallel keys and $k_{shp}=25\text{kg/mm}^3$ for segmented keys.

2.15. Error Due to Pinning Deformation

$\varphi_{sht}=k_{sht}\times M$, radian, where k_{sht} is the coefficient of proportionality, M is the moment on the shaft [9].

2.16. Total Gear Stiffness

$C = \left\{\sum_{j=1}^{n}\left[\frac{(\phi_{defl}+\phi_{tw}+\phi_{tooth}+\phi_{shp}+\phi_{sht})_j}{M_j\times i_j^2}\right]\right\}^{-1}, kg \times \text{т} \times rad$, where i is the gear ratio related to the input shaft.

2.17. Natural Frequency of the Design

$f = \frac{1}{\pi} \times \sqrt{\frac{C\times i_{total}^2}{J_5}}, Hz$, where i_{total} is the total gear ratio, C is the rigidity, and J_5 is the reduced moment of inertia.As a result, it is necessary to obtain the rigidity of gearboxes, bearings and gear rims. Next, approximate the bearings, gear rims and gearboxes by systems of rod systems of identical stiffness in the model. Characteristics of materials of carbon fiber, filler SAN Foam and magnesium alloy [17-19] are given in Tables 1-3. Table 4 shows the effect of the orientation of the layers of the 8-layer composite carrier layer. As seen from the Table 4, the most favorable location of the orientation of the layers in terms of strength corresponds to the last line of Table 4.

Table 1. Physical and mechanical characteristics of carbon fiber

Modulus of elasticity, MPa	Poisson's ratio	Shear modulus, MPa	Tensile strength, MPa	Ultimate compressive strength, MPa	Shear strength, MPa	Density, kg/m^3
$E_s=1.233\times10^5$	$\nu_{s\theta}=0.27$	$G_{s\theta}=0.5\times10^4$	$\sigma_s=1632$	$\sigma_s=704$	$\tau_{s\theta}=80$	1518
$E_\theta=0.778\times10^5$	$\nu_{\theta z}=0.42$	$G_{\theta z}=3.1\times10^3$	$\sigma_\theta=34$	$\sigma_\theta=68$	$\tau_{\theta z}=55$	
$E_z=0.778\times10^5$	$\nu_{sz}=0.27$	$G_{sz}=0.5\times10^4$	$\sigma_z=34$	$\sigma_z=68$	$\tau_{sz}=80$	

Table 2. Physical and mechanical characteristics of SAN Foam

Modulus of elasticity, MPa	Poisson's ratio	Shear modulus, MPa	Tensile strength, MPa	Shear sz, MPa	Shear θz, MPa	Density, kg/m^3
60	0.3	23	1.1	0.8	0.8	81

Table 3. Physical and mechanical characteristics of magnesium alloy

Modulus of elasticity (shear), MPa	Poisson's ratio	Density, kg/m^3	Tensile strength, compression, MPa	Tensile strength, compression, MPa
4.5×10^4 (1.6×10^4)	0.35	1740	250	190

Table 4. Influence of the orientation of composite material layers on the stress state

Orientation of layers, deg	1 layer	2	3	4	5	6	7	8
0/0/0/90/90/90/0/0	60.04	50.09	40.33	117.8	106.78	96.91	20.24	20.50
0/0/90/90/90/0/0/0	68.54	57.77	116.63	106.51	97.54	22.22	20.84	19.45
45/0/-45/0/0/-45/0/45	108.19	57.21	96.89	45.40	41.07	59.90	32.91	79.40
45/-45/90/45/0/-45/-45/45	69.05	82.86	130.45	43.73	87.99	38.98	51.75	65.67
0/0/0/45/-45/0/0/0	57.91	47.37	37.15	100.48	99.54	31.64	34.43	77.41
45/-45/3/45/-45/-3/-45/45	86.97	98.38	82.98	58.91	50.78	69.40	55.96	68.62
45/-45/5/45/-45/-5/-45/45	86.89	98.54	82.24	58.64	50.79	68.96	55.56	68.79
45/-45/10/-45/45/10/-45/45	86.27	98.82	79.39	57.58	50.45	67.17	54.73	68.02
0/15/30/-45/90/45/-30/0	64.02	43.07	51.63	78.34	155.90	73.85	45.62	42.58
45/-45/10/-45/45/-10/-45/45	91.25	90.84	78.75	58.49	40.98	66.02	58.00	64.30

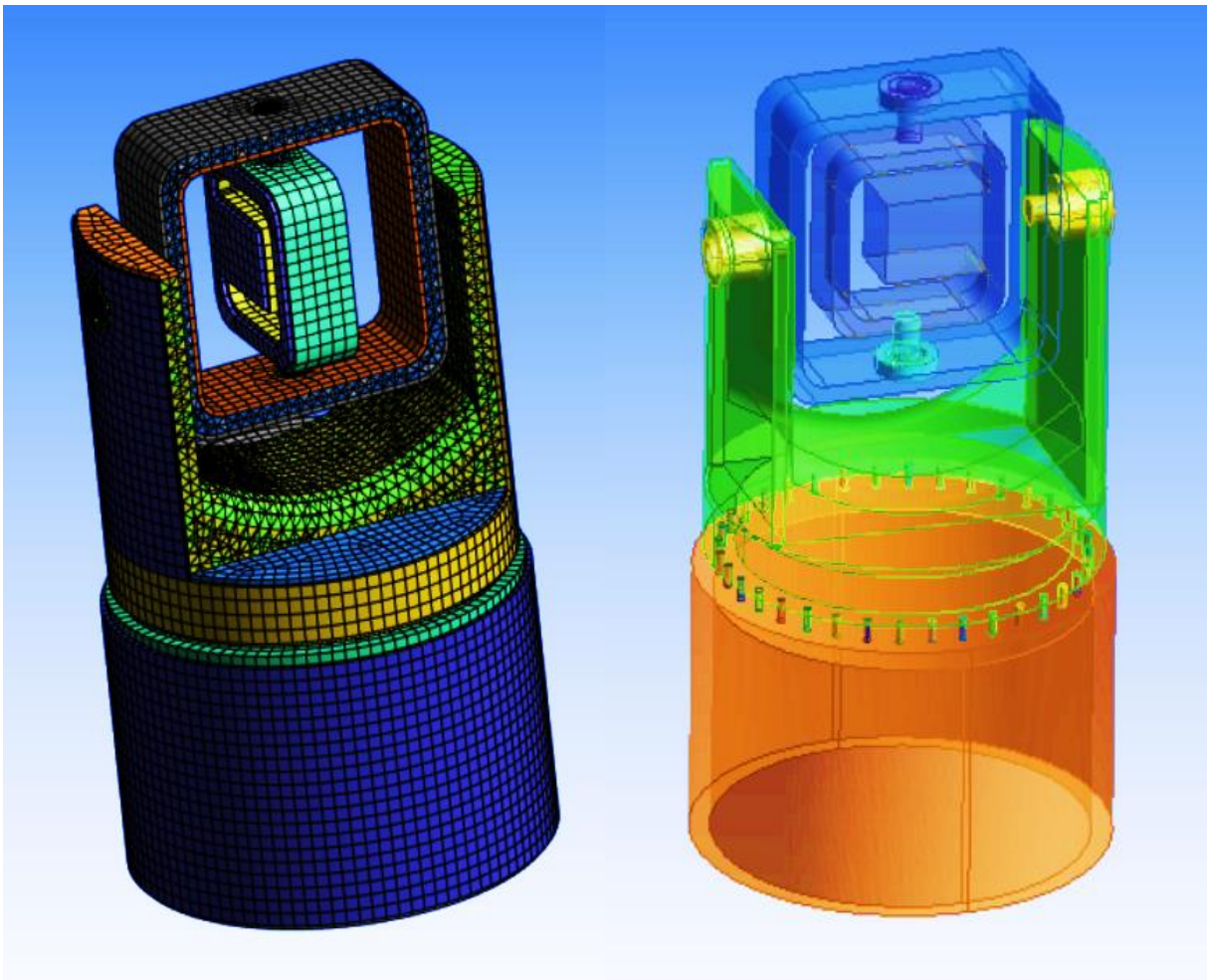

Fig. 3 Finite element approximation of the stand model and the stand with elements for approximating the bearings and the gear rim with a system of rod elements of identical rigidity

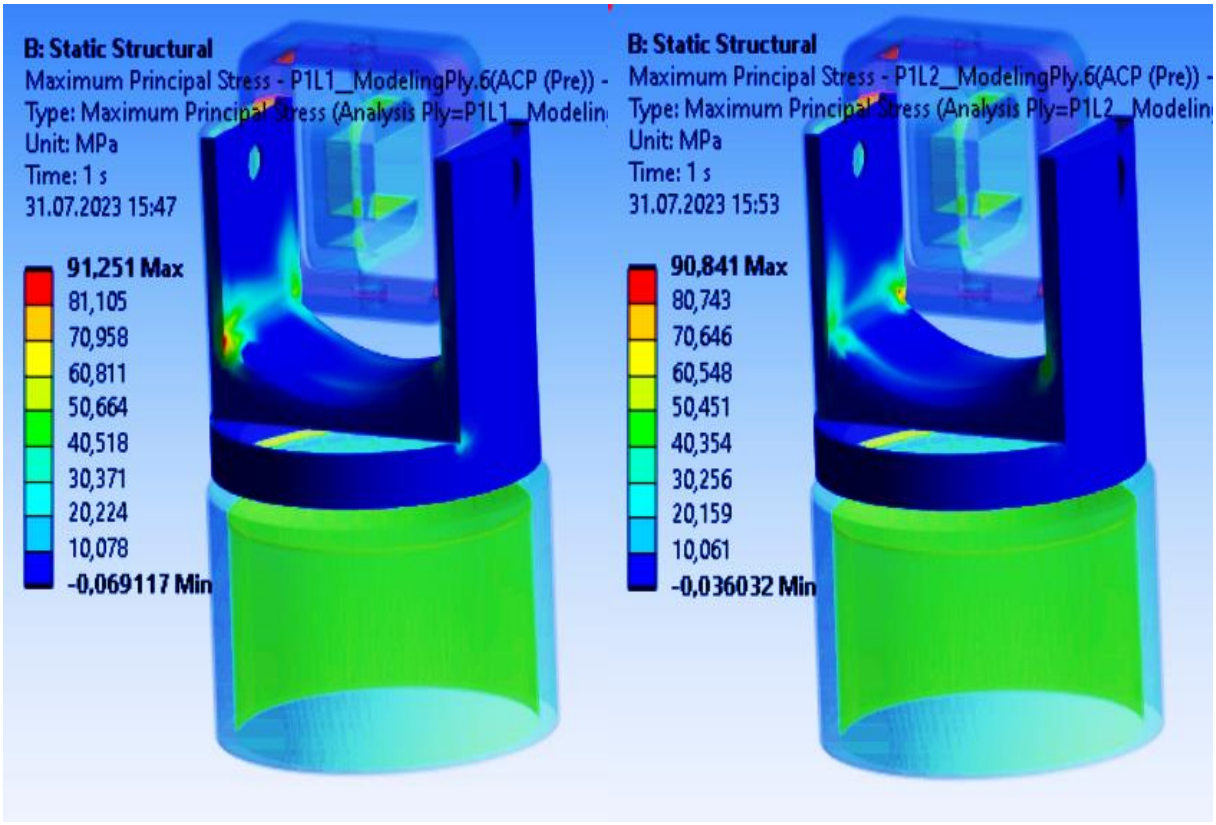

Fig. 4 Stresses in the first and the second layers of the composite material

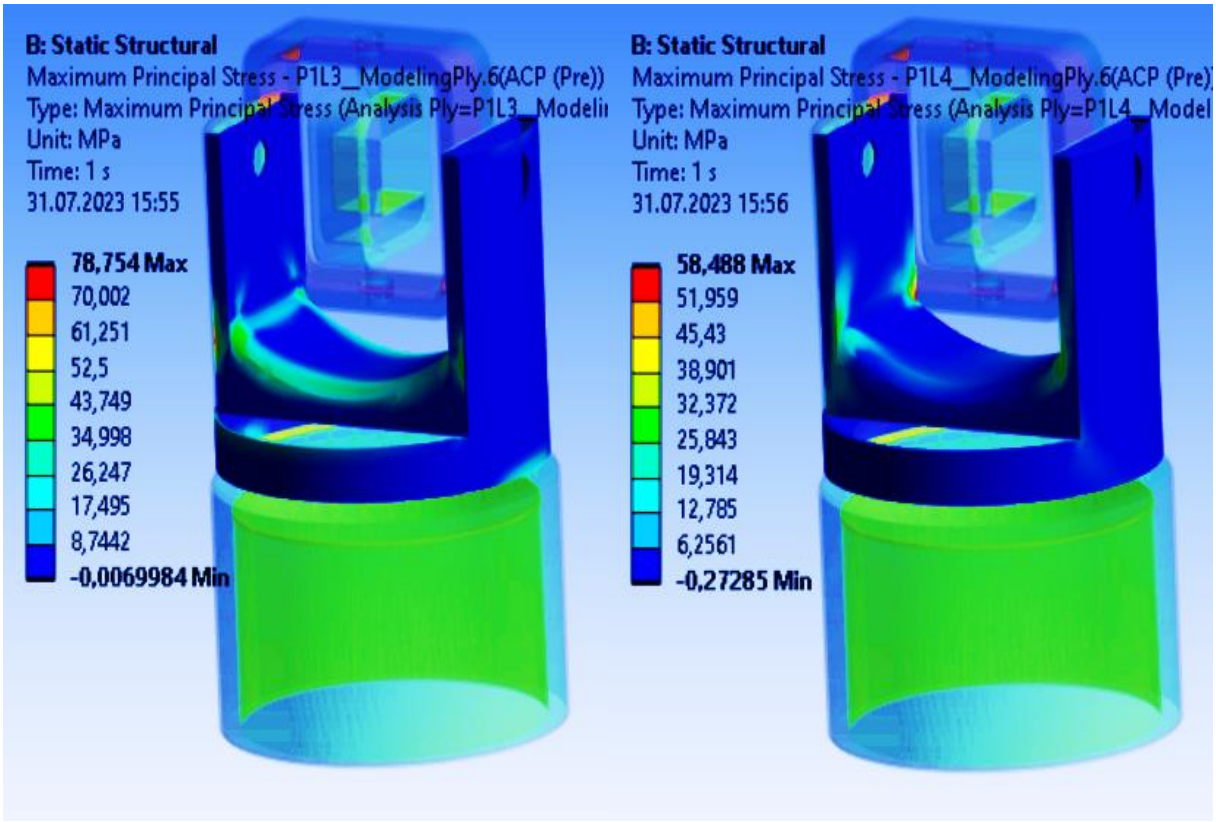

Fig. 5 Stresses in the third and the fourth layers of the composite material

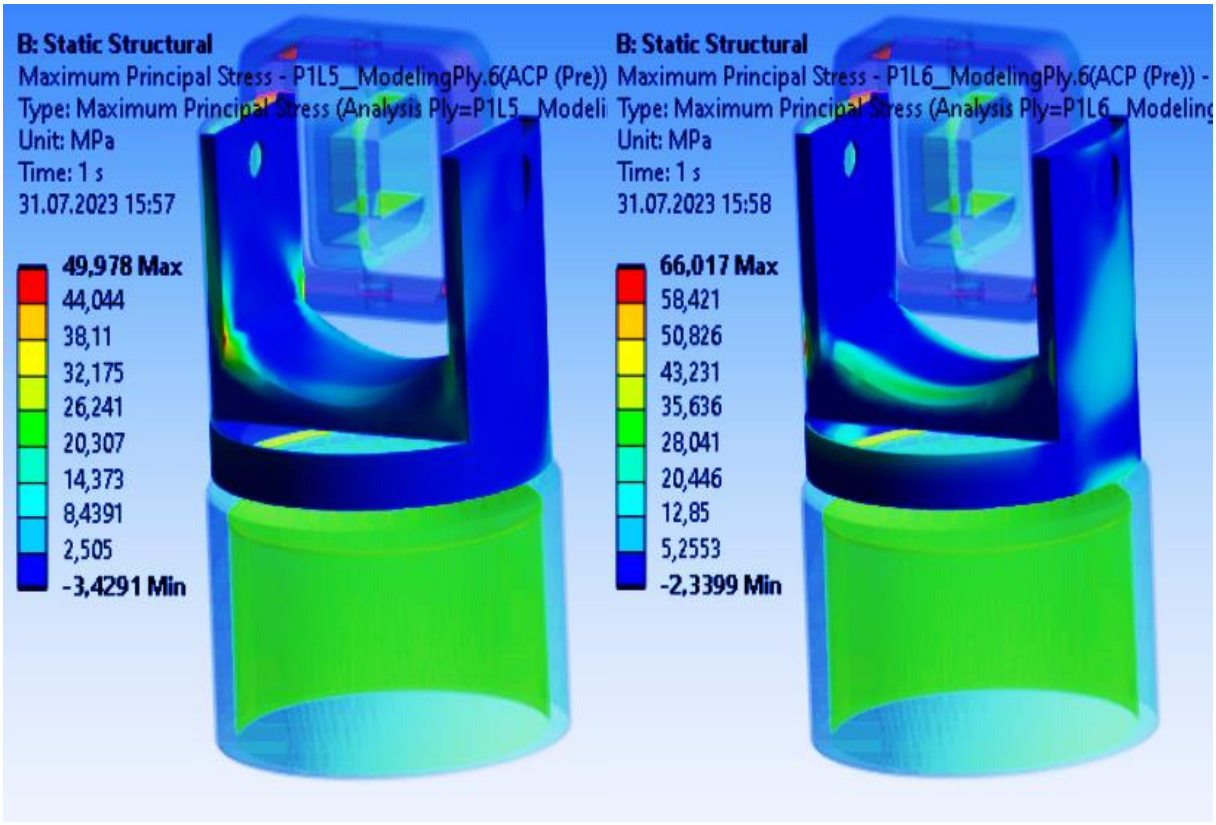

Fig. 6 Stresses in the fifth and the sixth layers of the composite material

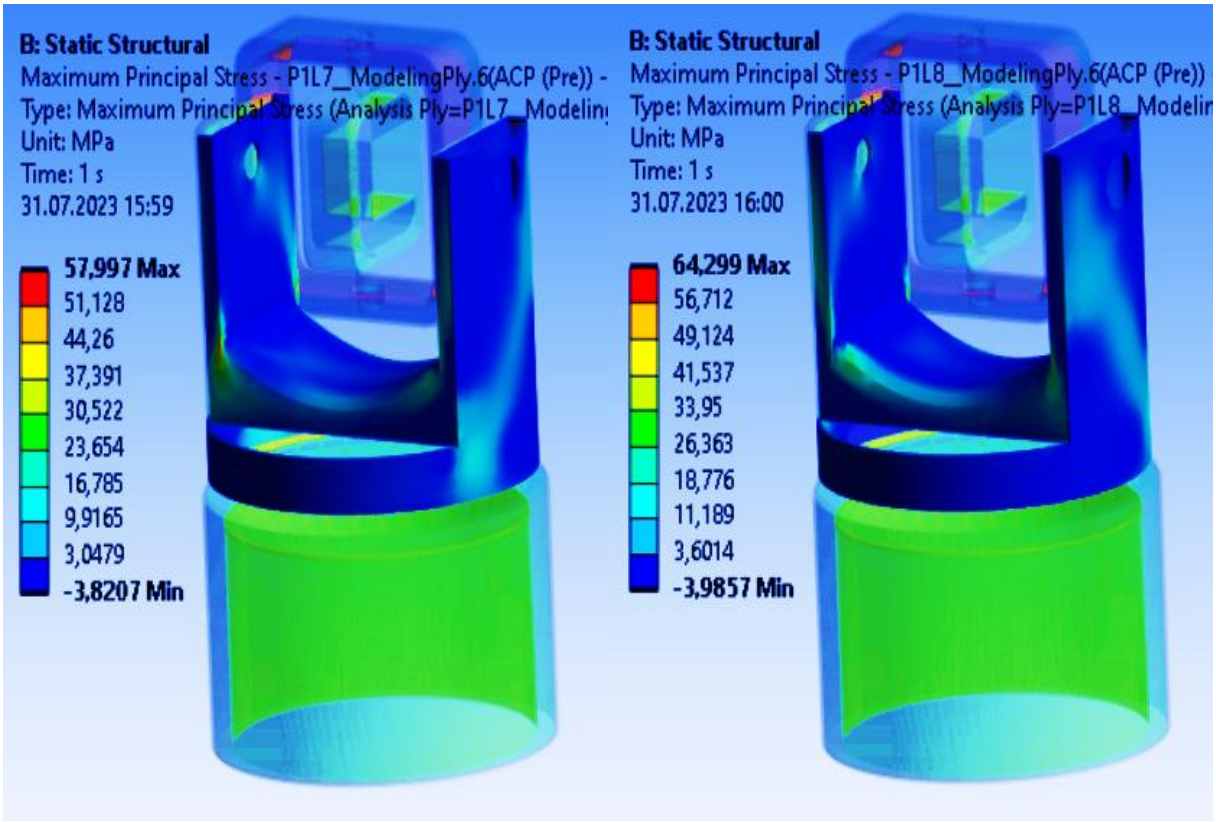

Fig. 7 Stresses in the seventh and the eighth layers of the composite material

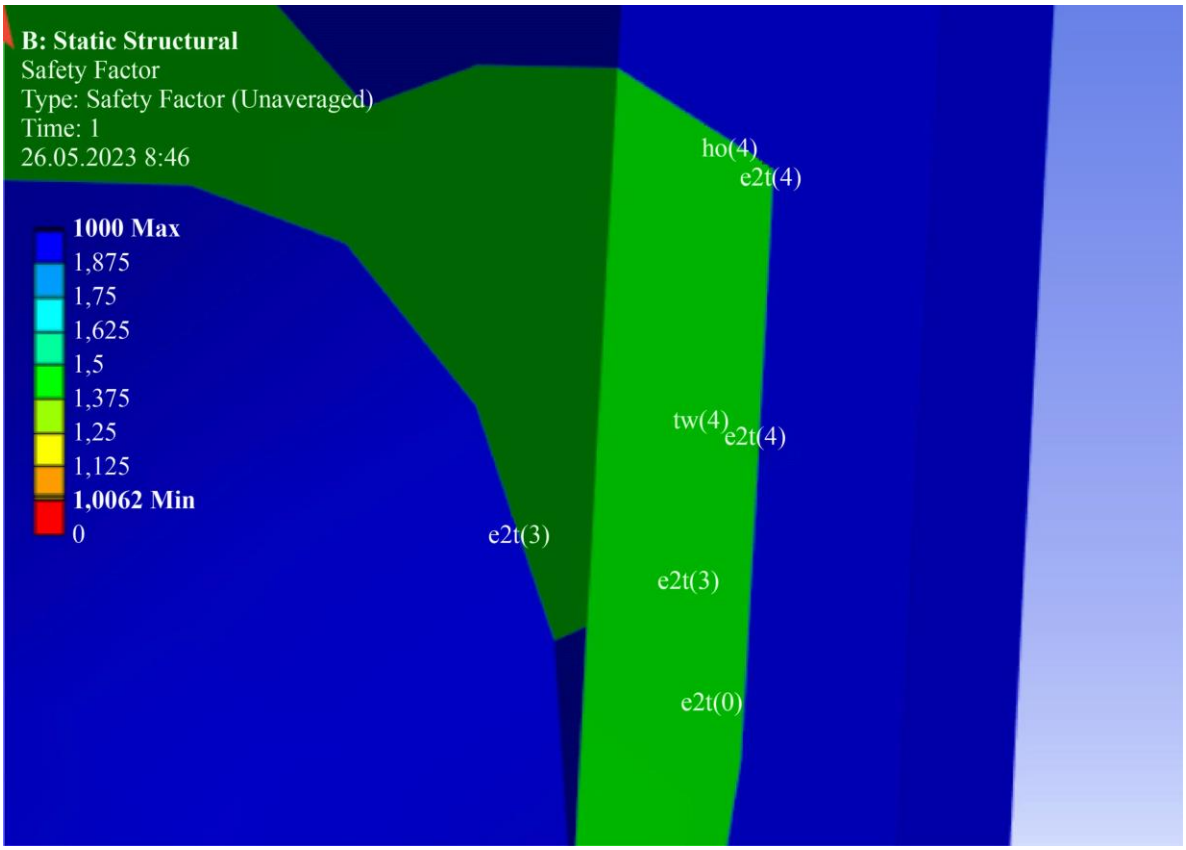

Fig. 8 Maximum stresses in a five-layer package: e - deformation, 2 - direction, t - tension, the number in brackets is the number of the layer, tw is the destruction of the layered structure according to the failure criterion of tw (Tsai-Wu) and ho (Hoffman)

3. Results and Discussion

The considered dynamic bench of semi-natural simulation is the three-stage slewing mechanism, consisting of a base, a course fork connected to it, and a pitch and roll ring included in the pitch ring. With the tested product installed in the roll ring, the stand makes movements in three degrees of freedom, simulating the operation of the product. When tested, the product moves through 3 degrees of freedom, simulating flight parameters in laboratory conditions. The use of dynamic stands makes it possible to reduce flight tests and thereby significantly reduce the cost of product testing. Figure 3 shows a general view of the stand approximated by finite elements and the stand with elements for approximating the bearings and the gear rim, a system of rod elements of identical rigidity. The rigidity of gearboxes and motors was considered in the rod system's rigidity. Figures 4-7 shows the stresses in the stand at an angular velocity of 500 deg/s, calculated at an angular velocity around the verti- o-axis of the channel, of course, and shows the stresses of a composite package of 8 unidirectional layers with a given orientation: 45/-45/10/-45/45/-10/-45/45 degrees layer by layer. Figure 8 shows the maximum stresses in a five-layer package: e - deformation, 2 - direction, t - tension; the number in brackets is the number of the layer, and tw and ho are the destructions of the layered structure according to the criterion of destruction of Tsai-Wu, Tsai-Hill and Hoffman criterion.

4. Conclusion

As a result of the work carried out, a three-layer dynamic stand was modeled. A three-layer structure was obtained by modeling the stand and assigning him the characteristics of the material (Table 2). Further, by modeling methods, external surfaces were created on the created model, assigned the characteristics of 8-layer composite material (Table 1). The location of the orientation of the layers of 8-layer composite material was obtained from the study. An algorithm and a program for calculating the rigidity of such structures as bearings, gear rims, and gearboxes have been developed to simulate the elements that provide movement of the bench channels. In the bench model, such elements were approximated by bar structures of identical rigidity. The legitimacy of such a replacement is confirmed by the comparisons made with the experimental data for calculating the natural frequencies of the stand. Calculations were carried out using the finite element method. The convergence of the obtained results was checked by condensing the finite element mesh and comparing the obtained results. To obtain a stand of maximum rigidity and strength, the base of the layers of the composite material was located relative to the trajectories of maximum stresses. These trajectories are obtained from solving the problem of the stress-strain state of the stand loaded with an angular operational velocity of 500 rad/s from a homogeneous material. In the future, the direction of the

trajectories of maximum stresses was corrected in the study of a stand made of composite material. Calculations were made of the influence of the orientation of the layers of 8-layer composite material on the stress state. The calculation results are summarized in Table 4. The reliability of the obtained results is confirmed by the use of programs tested on many examples, and the convergence of calculation results verified by refinement of the finite element mesh. Unfortunately, there are no methods in the literature for calculating the stress-strain state of robotic systems containing bearings, gears, gearboxes and motors in the structure, which are inadequately implemented in design schemes. There are only calculations of individual elements and parts made of composite materials.

This study proposes a method for calculating robotic systems by replacing elements that carry out movements with a system of rod structures of identical rigidity, taking into account rigidity not only in the plane of the bearing but also from the plane, more adequately taking into account the real rigidity of the structure. A method for calculating a robotic system made of a composite material, the characteristics of which depend on the location of the base layers in a multilayer composite material, is proposed.The calculation methods are developed and applied to a wide class of robotic systems with bearings, gear rims and gearboxes.

Funding Statement

Funding: This work was carried out with the financial support of the Russian Science Foundation under the scientific project No. 22-29-20299 (recipient Khayrnasov K.Z., https://rscf.ru/project/22-29-20299/).

References

[1] Yongding Tian et al., "Intelligent Robotic Systems for Structural Health Monitoring: Applications and Future Trends," *Automation in Construction*, vol. 139, 2022. [CrossRef] [Google Scholar] [Publisher Link]

[2] Baoxin Tao et al., "Accuracy of Dental Implant Surgery using Dynamic Navigation and Robotic Systems: An in Vitro Study," *Journal of Dentistry*, vol. 123, 2022. [CrossRef] [Google Scholar] [Publisher Link]

[3] P.W Singer, *Wired for War: The Robotics Revolution and Conflict in the 21st Century*, Penguin Publishing Group, pp. 1-512, 2009. [Google Scholar] [Publisher Link]

[4] Caroline Shackleton, and Nathan Paul Turner, *Robots: The Next Generation? Level B2+*, Cambridge Discovery Education, 2014. [Google Scholar] [Publisher Link]

[5] Mrinmoy Sarkar et al., "A Novel Search and Survey Technique for Unmanned Aerial Systems in Detecting and Estimating the Area for Wildfires," *Robotics and Autonomous Systems*, vol. 145, 2021. [CrossRef] [Google Scholar] [Publisher Link]

[6] H. Nagatani, "A New Resolution to Contact Problem of Roller Bearings," *The Tribology*, vol. 6, no. 346, pp. 44-46, 2016. [Google Scholar]

[7] Tedric A. Harris, and Michael N. Kotzalas, *Advanced Concepts of Bearing Technology: Rolling Bearing Analysis*, 5th ed., CRC Press, pp. 1-368, 2006. [Google Scholar] [Publisher Link]

[8] Peter R.N. Childs, *Rolling Element Bearings*, Mechanical Design Engineering Handbook, 2nd ed., UK: Elsevier Ltd, pp. 231-294, 2021. [CrossRef] [Google Scholar] [Publisher Link]

[9] Song Wang, and Yunyu Cao, "Analysis of Planetary Gear Transmission Characteristics Based on ANSYS," *Journal of Engineering Research and Reports*, vol. 23, no. 1, pp. 22-32, 2022. [CrossRef] [Google Scholar] [Publisher Link]

[10] Artem Voloshkin et al., "Comparison of Methods of Finite Element Analysis in the Design of Mobile Robot Modules," *IFToMM International Conference on Mechanisms, Transmissions and Applications*, pp. 254-263, 2023. [CrossRef] [Google Scholar] [Publisher Link]

[11] Isaac M. Daniel, "Yield and Failure Criteria for Composite Materials Under Static and Dynamic Loading," *Progress in Aerospace Sciences*, vol. 81, pp. 18-25, 2016. [CrossRef] [Google Scholar] [Publisher Link]

[12] A. Puck, and H. Schürmann, "Failure Analysis of FRP Laminates by Means of Physically based Phenomenological Models," *Composites Science and Technology*, vol. 62, no. 12-13, pp. 1633-1662, 2002. [CrossRef] [Google Scholar] [Publisher Link]

[13] D. Rajpal et al., "Design and Testing of Aeroelastically Tailored Composite Wing Under Fatigue and Gust Loading Including Effect of Fatigue on Aeroelastic Performance," *Composite Structures*, vol. 275, 2021. [CrossRef] [Google Scholar] [Publisher Link]

[14] A.M Mirzaei et al., "Fatigue Life Assessment of Notched Laminated Composites: Experiments and Modelling by Finite Fracture Mechanics," *Composites Science and Technology*, vol. 246, 2024. [CrossRef] [Google Scholar] [Publisher Link]

[15] O.G. Latyshev, A.B. Veremeychik, and E.A. Zhukov, *Application of Composite Materials in Stands for Dynamic Loading*, Moscow, Publishing house of MSTU NE Bauman, 2011. [Google Scholar]

[16] Spyridon Kilimtzidis et al., "Modeling, Analysis and Validation of the Structural Response of a Large-Scale Composite Wing by Ground Testing," *Composite Structures*, vol. 312, 2023. [CrossRef] [Google Scholar] [Publisher Link]

[17] Vaibhav A. Phadnis, and Vadim V Silberschmidt, "8.14 Composites Under Dynamic Loads at High Velocities," *Comprehensive Composite Materials II*, vol. 8, pp. 262-285, 2018. [CrossRef] [Google Scholar] [Publisher Link]

[18] Pablo Castelló-Pedrero, César García-Gascón, and Juan A. García-Manrique, "Multiscale Numerical Modeling of Large-Format Additive Manufacturing Processes using Carbon Fiber Reinforced Polymer for Digital Twin Applications," *International Journal of Material Forming*, vol. 17, no. 2, pp. 1-14, 2024. [CrossRef] [Google Scholar] [Publisher Link]

[19] A. Manes et al., "Experimental and Numerical Investigations of Low Velocity Impact on Sandwich Panels," *Composite Structures*, vol. 99, pp. 8-18, 2013. [CrossRef] [Google Scholar] [Publisher Link]

[20] Narendra Kumar Jha et al., "Finite Element and Micromechanical Analysis of Glass/Epoxy Laminated Composite with Different Orientations," *MaterialsToday: Proceedings*, vol. 28, pp. 1899-1903, 2020. [CrossRef] [Google Scholar] [Publisher Link]

[21] Jian-Ping Lin et al., "Static and Dynamic Analysis of Three-Layered Partial-Interaction Composite Structures," *Engineering Structures*, vol. 252, 2022. [CrossRef] [Google Scholar] [Publisher Link]

[22] Qian Guo et al., "Constitutive Models for the Structural Analysis of Composite Materials for the Finite Element Analysis: A Review of Recent Practices," *Composite Structures*, vol. 260, 2021. [CrossRef] [Google Scholar] [Publisher Link]

[23] Wael Al-Tabey, *Introduction to Composite Materials for Engineering*, Lambert Academic Publishing, pp. 1-124, 2012. [Google Scholar] [Publisher Link]

[24] Haowei Huang, S. Ali Hadigheh, and Keyvan Aghabalaei Baghaei, "Influences Of Fibre Shape On The Transverse Modulus Of Unidirectional Fibre Reinforced Composites Using Finite Element And Machine Learning Methods," *Composite Structures*, vol. 312, 2023. [CrossRef] [Google Scholar] [Publisher Link]

[25] Christos Kassapoglou, *Design and Analysis of Composite Structures: With Applications to Aerospace Structures*, Wiley, pp. 1-314, 2010. [Google Scholar] [Publisher Link]

[26] Olek C. Zienkiewicz, Robert L. Taylor, and J.Z. Zhu, *The Finite Element Method: Its Basis and Fundamental*, Elsevier Science, pp. 1-756, 2013. [Google Scholar] [Publisher Link]

[27] V.P. Radin, Yu.N. Samogin, and V.P.Chirkov, *Finite Element Method in Dynamic Problems of Strength of Materials*, Moscow, Russia: FIZMATLIT, 2013. [Google Scholar] [Publisher Link]

[28] Ioannis Koutromanos, *Fundamentals of Finite Element Analysis: Linear Finite Element Analysis*, Wiley, pp. 1-710, 2018. [Google Scholar] [Publisher Link]

[29] Klaus-Jürgen Bathe, "*Finite Element Procedures*," Prentice Hall, pp. 1-1037, 2006. [Google Scholar] [Publisher Link]